Binary to quaternary Mo-based phosphate glasses cathodes Li-batteries: Influence of Mo substitution by Fe and Mn

DELANOE, Alexis, AGULLO, Julia, DE ARAUJO, Maxime, GUYOT, Taos, MUCCI, Romain, PERRET, Damien, SIMONIN, Loic and MARTINET, Sébastien

Materials Letters 382 (2025) 137879

Contents lists available at ScienceDirect

Materials Letters

journal homepage: www.elsevier.com/locate/matlet

Binary to quaternary Mo-based phosphate glasses cathodes Li-batteries: Influence of Mo substitution by Fe and Mn

Alexis Delanoë [a], Julia Agullo [b], Maxime De Araujo [b], Taos Guyot [a,b], Romain Mucci [a], Damien Perret [b], Loic Simonin [a], Sébastien Martinet [a,*]

[a] Université Grenoble Alpes, CEA, Liten, DEHT, 38000 Grenoble, France
[b] CEA, DES, ISEC, DPME, Univ. Montpellier, Marcoule, France

ARTICLE INFO

Keywords:
Phosphate glass
Cathode
Positive electrode
Li-ion batteries
Design of Experiment

ABSTRACT

To correlate glass chemical compositions with electrochemical performances, seven Mo-phosphate glasses (with/without Fe and/or Mn) were prepared using a Design of Experiment approach and characterized (XRD, EDS, XRF). Evaluated as cathode active materials in Li-metal coin cells, their electrochemical performances were measured by galvanostatic cycling at C/50 rate. The glasses show high first discharge capacities, but energy densities (420 to 705 Wh/kg at the material level) were limited by low voltage. Significant capacities losses (≈50%) occured between the first and second discharges, affecting subsequent performances. Ternary diagrams for first cycles discharge capacities and voltage are presented.

1. Introduction

Development of new positive electrode materials (or cathode) for Li-ion batteries is a challenge to improve batteries performances. Most current cathodes are crystalline materials, while amorphous materials, such as glasses, are less studied. Glasses, being structurally tolerant, allow lithium insertion/deinsertion within their matrix [1]. Their amorphous network can theoretically incorporate high amount of transition metal oxide, potentially achieving high specific capacities.

Most of glass cathodes studies focus on Vanadium-containing systems [2], due to Vanadium's glass forming element behavior and versatile oxidation states (+III, +IV or + V), providing high electrochemical energy density up to 1000 Wh/kg at the material level [3]. However, Vanadium is toxic and classified as critical element by European Union. Vanadium-free glass cathodes are rarely reported in the literature [4–7], but Wu *et al.* [8] observed notable initial discharge capacities (300 mAh/g) for unlithiated MoO_3-P_2O_5 glasses, associated with significant capacity losses in subsequent cycles.

MoO_3 is an expensive transition metal oxide, so this study explores its substitution with Fe_2O_3 and MnO_2. Optimal MoO_3-Fe_2O_3-MnO_2-P_2O_5 glass compositions were determined using a Design of Experiment (DOE) approach in order to determine correlations between chemical compositions and electrochemical performances. The glasses were synthetized through melt-quenching method and characterized by galvanostatic cycling.

2. Materials and methods

Seven glass chemical compositions were selected using an augmented simplex lattice DOE (Fig. 1(b)). Constraints were set up from molar contents (Fig. 1(a)). As preliminary results led to crystallization during air-quenching for lower P_2O_5 contents in the glass formulation, P_2O_5 was fixed at 40 $\%_{mol.}$. MoO_3 was ranged from 30 to 60$\%_{mol.}$ to minimize cost, keeping relatively high theoretical specific capacities. This work studies inexpensive and less critical materials with Fe_2O_3 and MnO_2 incorporation, these two components were ranged from 0 to 30$\%_{mol.}$ to make 100$\%_{mol.}$ total.

Seven glass compositions defined by the DOE were synthetized using melt-quenching method. Precursors (Sigma-Aldrich: MoO_3, >99.98 %; Fe_2O_3, >96 %; MnO_2, >99 %; P_2O_5, >99 %) were mixed in an alumina crucible. The thermal protocol involved heating from room temperature up to 1200 °C at 5 °C/min, with a 1-hour dwell at 350 °C and a second one at 1200 °C. The melting glasses were then quenched on copper plate in air, cooled and crushed with a pestle in a mortar.

The amorphous structure of each glass was verified using powder X-ray diffraction diffractometer (XRD), with Cu-Kα radiation (λ = 0.154 nm) in the range of 2θ = 10-80° (Bruker D8 advance diffractometer, Diffrac.Eva analysis software). Chemical homogeneity was checked

* Corresponding author.
E-mail address: sebastien.martinet@cea.fr (S. Martinet).

https://doi.org/10.1016/j.matlet.2024.137879
Received 27 August 2024; Accepted 9 December 2024
Available online 10 December 2024

through Scanning Electronic Microscopy Energy Dispersive X-ray, SEM-EDX (ZEISS Sigma 300E, Oxford Ultim Max 170). EDX results were analyzed using Aztec V5.0 SP1 software. Chemical composition was determined by X-ray fluorescence spectroscopy, XRF (Bruker S8 TIGER Series 2), using fused bead glass samples prepared by melting 0.5 g of glass with 9.5 g of lithium borate mixture at 1200 °C, using XRF scientific xrFuse 1 machine.

The positive electrode was made by mixing 80 $\%_{wt.}$ of glass powder, 10 $\%_{wt.}$ of nanometric black carbon (Super C65, Timcal®), and 10 $\%_{wt.}$ of polyvinylidene fluoride binder (Solef® 5120/1001) with N-Methyl-2-Pyrrolidone solvent (>99.7 %, Supelco®). This ink was deposited on an aluminium foil with a Doctor blade coater set to 100-µm thickness, and dried at 60 °C overnight to remove solvent. Electrode pellets (Ø=14 mm) were pressed at 10 tons in a hydrolic press to reduce porosity and improve electronic percolation. These electrodes were assembled into coin cell inside an argon glove box ($[H_2O]$ and $[O_2] < 1$ ppm) using 1 M $LiPF_6$ in $1_{vol.}/1_{vol.}/3_{vol.}$ EC/PC/DMC (Ethylene Carbonate/Propylene Carbonate/Dimethyl Carbonate) electrolyte from UBE Industries, Celgard separator, Viledon electrolyte reservoir and Li-metal anode.

Theoretical capacities (Table 1) were estimated based on theoretical compositions, assuming 1 electron exchange for Mn, 2 for Fe, and 3 for Mo. Galvanostatic cycling was performed on an ARBIN test bench, between 1 V and 4.7 V, at C/50 rate (i.e. ≈5.1 to 6.7 mA/g), starting with discharge.

3. Results and discussion

3.1. Glass synthesis and characterizations

After syntheses, the glasses' amorphous structure were confirmed by XRD. No diffraction peaks were observed indicating glass formation (Fig. 2(a)). Despite P_2O_5 being hygroscopic, the measured contents determined by XRF (Table 1) are similar to the theoretical values, usually within XRF uncertainty (±10 $\%_{mol.}$). Using $(NH_4)_2HPO_4$ precursor could reduce P variations as this precursor is not hygroscopic. Furthermore, variabilities in MoO_3, MnO_2 and Fe_2O_3 contents could be due to precursor evaporation. Adapted thermal treatment could reduce variabilities.

Chemical homogeneity was confirmed by SEM-EDX with an example for the 35Mo-20Fe-5Mn-40P glass shown on the Fig. 2(c).

3.2. Electrochemical behavior

Glass electrochemical performances were evaluated by applying a constant current until voltage limit were reached, with voltage measured during charging and discharging at low rate. As glasses are lithium-free, galvanostatic cycling began with discharge (i.e. negative current application resulting in decrease of the cell voltage), to incorporate lithium from Li metallic anode into the glass cathode. During charging (i.e. positive current application resulting in a voltage increase) lithium was extracted from the glass cathode and deposited on the anode. The first, second, fifth and tenth cycles of all glasses are presented on the Fig. 3(a)–(g).

For every glass, the first discharge curve shows a high specific capacity typically above 385 mAh/g (compared with 120 to 200 mAh/g for commercial cathode materials). However, a high irreversible capacity loss associated with significant change of the electrochemical curve shape suggest a possible irreversible structural modification during the first cycle. A first horizontal discharge plateau between 1 and 2.5 V, may indicate conversion reactions, as observed on crystalline anodes materials [9], leading to metal formation. Another hypothesis would be the formation of Li_2MoO_4 phases, as observed in high MoO_3 content glasses [8]. Fe_2O_3 and/or MnO_2 may also contribute to phase formation. A similar capacity loss around 50 % is obtained across DOE glass compositions (Table 1, Fig. 3(h)). For example, the 35Mo-20Fe-5Mn-40P glass has a first discharge capacity of 494.9 mAh/g, dropping of 42.8 % down to 282.9 mAh/g after the second discharge (Fig. 3(e)).

Wu *et al.* [8] previously observed this irreversible phenomena in binary Mo-P glasses, likely due to lithium trapping in the glass structure/network causing structural changes. Another hypothesis is that the

Component	$\%_{mol.}$ min.	$\%_{mol.}$ max.
MoO_3	30%	60%
Fe_2O_3	0%	30%
MnO_2	0%	30%
P_2O_5	constant = 40%	

a)

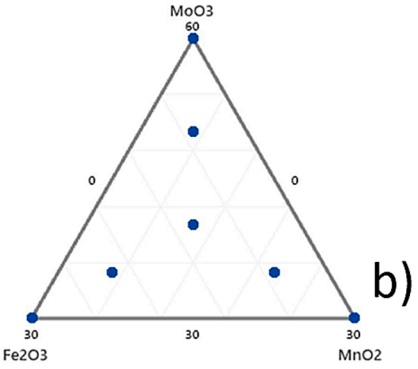

b)

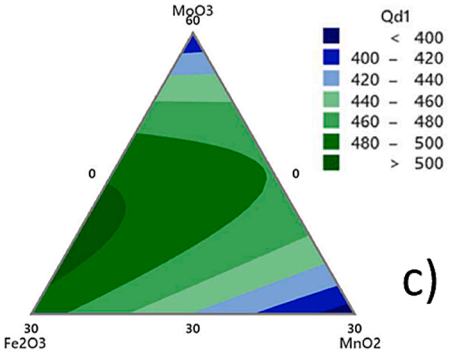

c)

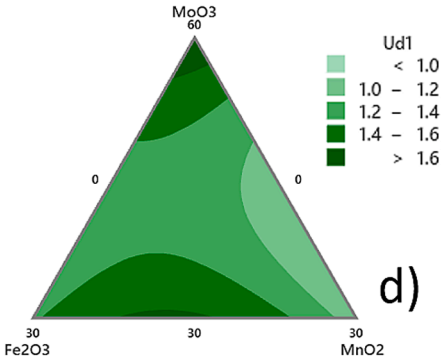

d)

Fig. 1. Seven glasses compositions defined by DOE (b), with DOE components limits (a). Ternary diagrams of first specific capacity (c) and first discharge voltage (d) generated by DOE. $r^2(Q_{disch.1})=0.9922$ and $r^2(U_{disch.\ 1})=0.9999$.

Table 1
Theoretical glass chemical compositions suggested by DOE, and XRF determined chemical compositions. Glasses electrochemical performances at the first and the second discharge, determined by galvanostatic cycling.

Sample name	Theoretical composition ($\%_{mol.}$)				Chemical composition ($\%_{mol}$,XRF)				Electrochemical performances							
	MoO_3	Fe_2O_3	MnO_2	P_2O_5	MoO_3	Fe_2O_3	MnO_2	P_2O_5	$Q_{th.}$ (mAh/g)	$Q_{disch.1}$ (mAh/g)	$Q_{disch.2}$ (mAh/g)	$U_{disch.1}$ (V vs Li^+/Li)	$U_{disch.2}$ (V vs Li^+/Li)	$E_{disch.1}$ (Wh/kg_{AM})	$E_{disch.2}$ (Wh/kg_{AM})	Loss between $Q_{disch.1}$ and $Q_{disch.2}$
40 Mo-10Fe-10Mn-40P	40 %	10 %	10 %	40 %	39.6 %	13.1 %	6.5 %	40.8 %	289	453.9	275.2	1.32	1.36	597.9	375.2	39.4 %
30Mo-30Mn-40P	30 %	–	30 %	40 %	37.6 %	–	20.1 %	42.3 %	255	386.4	145.3	1.09	1.11	420.1	161.0	62.4 %
60Mo-40P	60 %	–	–	40 %	66.1 %	–	–	33.9 %	337	398.8	207.0	1.79	1.70	713.7	351.8	48.1 %
50Mo-5Fe-5Mn-40P	50 %	5 %	5 %	40 %	53.7 %	6.0 %	3.0 %	37.3 %	313	476.5	264.7	1.38	1.52	655.2	403.4	44.4 %
35Mo-20Fe-5Mn-40P	35 %	20 %	5 %	40 %	38.9 %	19.8 %	2.6 %	38.7 %	280	494.9	282.9	1.42	1.45	701.1	409.3	42.8 %
35Mo-5Fe-20Mn-40P	35 %	5 %	20 %	40 %	40.2 %	9.5 %	11.2 %	39.1 %	273	454.4	227.8	1.24	1.28	563.7	292.6	49.9 %
30Mn-30Fe-40P	30 %	30 %	–	40 %	23.6 %	34.6 %	–	41.8 %	272	464.5	250.2	1.52	1.57	704.9	392.0	46.1 %

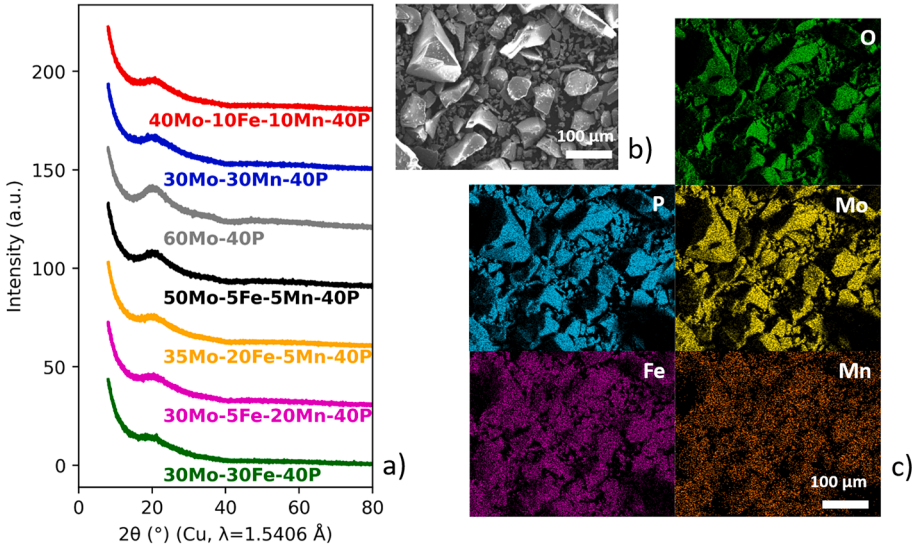

Fig. 2. XRD diffractograms of the seven glasses (a). Example of SEM (b) and EDX cartography analyses (c) performed at 15 kV on 35Mo-20Fe-5Mn-40P glass.

particle size distribution (PSD) affects lithium diffusion kinetic during charge and discharge. Larger glass particles lengthen the lithium diffusion path, requiring more time for insertion and extraction. Our glasses currently have a PSD of around 100 µm (not shown) that could be reduced to decrease capacity loss.

3.3. Performance optimization using DOE

Electrochemical performances were analyzed using DOE to identify main effects and potential interactions. Ternary diagrams for the predicted first discharge specific capacity and voltage were created (Fig. 1 (c) and (d)). Fig. 1(c) shows that, with a constant 40 $\%_{mol.}$ P_2O_5 content, high initial discharge capacities (>500 mAh/g) could occur with low MnO_2 content (≤3.1 $\%_{mol.}$), intermediate Fe_2O_3 content (15.9 $\%_{mol.}$-27 $\%_{mol.}$) and high MoO_3 content (32.9 $\%_{mol.}$-44 $\%_{mol.}$). However, these high discharge capacities correspond to a low voltage zone (1 to 1.2 V, Fig. 1(d)), limiting energy densities. The voltage diagram indicates that high MoO_3 content (≈60 $\%_{mol.}$) can lead to higher voltage (>1.6 V), typical of MoO_3-P_2O_5 glass.

In our study, the first mean discharge voltage remains low (<2V), compared to typical cathodes (3 to 4 V). As the voltage is highly dependent on the components of the active materials, the voltage could be increased by selecting other transition metals or substituting the phosphate anion to modify inductive effect [11]. Therefore, despite high first discharge capacities, our first measured energy densities ranges from 420 to 705 Wh/kg at the material level (Table 1), which are moderate but encouraging for Vanadium-free glasses cathodes development up to 1000 Wh/kg. Furthermore, capacity loss leads to decrease energy in the second discharge, despite stable voltage between the two cycles.

4. Conclusion and perspectives

To our knowledge, this study is the first to incorporate Mn and/or Fe into Mo-phosphate glasses using a DOE approach for battery application. Initial discharge capacity are promising, but performance is limited by

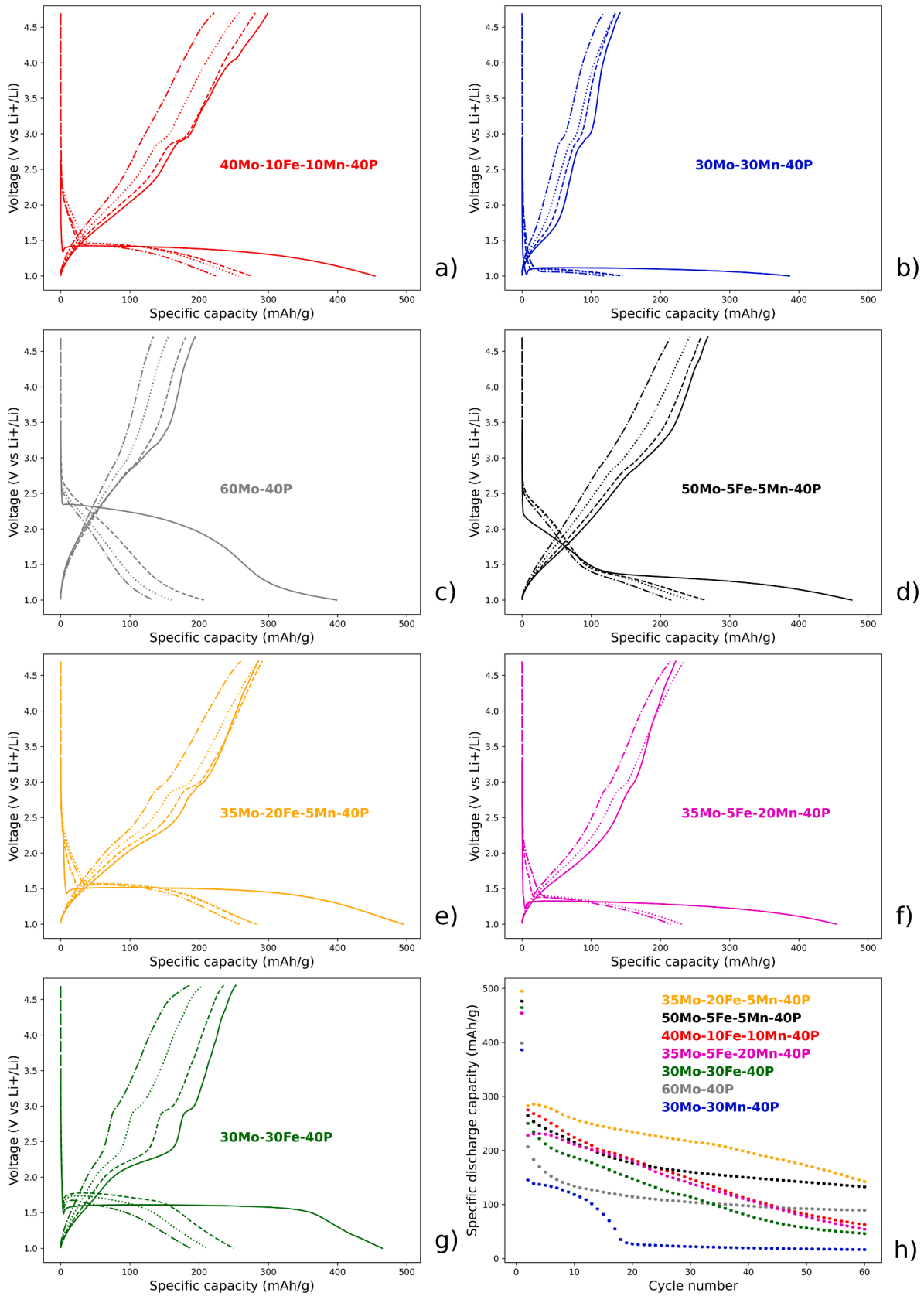

Fig. 3. Galvanostatic cycling of the seven glasses. First cycle (continuous line), the 2nd cycle (dashed line), the 5th cycle (dotted line) and the 10th cycle (dashed-dotted line). Seven glasses discharge specific capacities evolution through the cycling (h).

capacity loss in the second cycle. At the material level, discharge energy density is moderate (420 to 705 Wh/kg) mainly due to low average discharge voltage. Optimization of electrode formulation is another strategy to improve electrochemical performances, enhancing its conductivity.

DOE helped create electrochemical performances ternary diagrams linked to chemical compositions. It could be interesting to use the predictive capability of the DOE models to explore additional compositions and to optimize responses.

Additional characterizations could reveal underlying mechanisms. *Post-mortem* structural characterizations will study glass network or identify phases formation (Raman spectroscopy, XRD, or X-Ray Photoelectron Spectroscopy). Determining oxidation state (XPS, X-ray Absorption Near Edge Structure) is crucial to understand performance. Conductivity measurement (chronoamperometry and electrochemical impedance spectroscopy [10]) will determine ionic and electrical conductivities. These results will be added to a database to correlate chemical composition, glass properties and electrochemical performances.

CRediT authorship contribution statement

Alexis Delanoë: Formal analysis, Investigation, Methodology, Writing – original draft, Writing – review & editing, Software, Validation. **Julia Agullo:** Investigation, Methodology, Resources, Supervision, Validation, Writing – original draft, Writing – review & editing, Formal analysis. **Maxime De Araujo:** Formal analysis, Investigation, Methodology, Writing – review & editing, Validation. **Taos Guyot:** Formal analysis, Investigation, Methodology, Writing – review & editing, Validation. **Romain Mucci:** Conceptualization, Formal analysis, Investigation, Methodology, Writing – review & editing, Validation. **Damien Perret:** Formal analysis, Investigation, Methodology, Supervision, Writing – review & editing, Visualization. **Loic Simonin:** Formal analysis, Investigation, Methodology, Supervision, Writing – review & editing, Validation. **Sébastien Martinet:** Conceptualization, Formal analysis, Funding acquisition, Investigation, Methodology, Project administration, Resources, Software, Supervision, Writing – original draft, Writing – review & editing, Validation.

Declaration of competing interest

The authors declare that they have no known competing financial interests or personal relationships that could have appeared to influence the work reported in this paper.

Data availability

Data will be made available on request.

References

[1] M. Kindle, Y. Cha, J.S. McCloy, M.-K. Song, Alternatives to Cobalt: Vanadate Glass and Glass-Ceramic Structures as Cathode Materials for Rechargeable Lithium-Ion Batteries, ACS Sustainable Chem. Eng. 9 (2021) 629–638, https://doi.org/10.1021/acssuschemeng.0c04026.

[2] Z. Wang, S. Luo, X. Zhang, S. Guo, P. Li, S. Yan, Glass and glass ceramic electrodes and solid electrolyte materials for lithium ion batteries: A review, J. Non Cryst. Solids 619 (2023) 122581, https://doi.org/10.1016/j.jnoncrysol.2023.122581.

[3] S. Afyon, F. Krumeich, C. Mensing, A. Borgschulte, R. Nesper, New High Capacity Cathode Materials for Rechargeable Li-ion Batteries: Vanadate-Borate Glasses, Sci Rep 4 (2014) 7113, https://doi.org/10.1038/srep07113.

[4] T. Togashi, T. Honma, K. Shinozaki, T. Komatsu, Electrochemical performance as cathode of lithium iron silicate, borate and phosphate glasses with different Fe2+ fractions, J. Non Cryst. Solids 436 (2016) 51–57, https://doi.org/10.1016/j.jnoncrysol.2016.02.001.

[5] M. Isono, S. Okada, J. Yamaki, Synthesis and electrochemical characterization of amorphous Li–Fe–P–B–O cathode materials for lithium batteries, J. Power Sources 195 (2010) 593–598, https://doi.org/10.1016/j.jpowsour.2009.07.038.

[6] J. Lomon, J. Padchasri, A. Montreeuppathum, S. Siriroj, N. Chanlek, Y. Poo-arporn, S. Pinitsoontorn, P. Songsiriritthigul, P. Kidkhunthod, Nickel and manganese on lithium borate glass cathode for energy storage materials, Materialia 26 (2022) 101583, https://doi.org/10.1016/j.mtla.2022.101583.

[7] S. Siriroj, J. Padchasri, A. Montreeuppathum, J. Lomon, N. Chanlek, Y. Poo-arporn, P. Songsiriritthigul, S. Pinitsoontorn, S. Rujirawat, P. Kidkhunthod, New glass cathode materials for Li-ion battery: Ni-Co doping in Li-B-O based glass, Mater. Sci. Energy Technol. 6 (2023) 554–560, https://doi.org/10.1016/j.mset.2023.05.005.

[8] X. Wu, S.-X. Zhao, L.-Q. Yu, J.-W. Li, E.-L. Zhao, C.-W. Nan, Lithium storage behavior of MoO3–P2O5 glass as cathode material for Li-ion batteries, Electrochim. Acta 297 (2019) 872–878, https://doi.org/10.1016/j.electacta.2018.12.039.

[9] J. Zhang, J. Zhang, J. Liu, Y. Cao, C. Huang, G. Ji, Z. Zhao, X. Ou, B. Zhang, Environmentally phase-controlled stratagem for open framework pyrophosphate anode materials in battery energy storage, J. Mater. Chem. C 9 (2021) 9147–9157, https://doi.org/10.1039/D1TC02106K.

[10] B.V.R. Chowdari, K.L. Tan, W.T. Chia, R. Gopalakrishnan, Thermal, physical, electrical and XPS studies of the Li2O: P2O5:MoO3 glass system, J. Non Cryst. Solids 126 (1991) 18–29, https://doi.org/10.1016/0022-3093(91)90773-Y.

[11] C. Masquelier, L. Croguennec, Polyanionic (Phosphates, Silicates, Sulfates) Frameworks as Electrode Materials for Rechargeable Li (or Na) Batteries, Chem. Rev. 113 (2013) 6552–6591, https://doi.org/10.1021/cr3001862.